

Strong interaction effects in high- Z K^- atoms

C. J. Batty,^a M. Eckhause,^b K. P. Gall,^{c,*} P. P. Guss,^{b,†} D. W. Hertzog,^{b,‡} J. R. Kane,^b
A. R. Kunselman,^d J. P. Miller,^c F. O'Brien,^{c,§} W. C. Phillips,^{b,**} R. J. Powers,^{e,††}
B. L. Roberts,^c R. B. Sutton,^f W. F. Vulcan,^b R. E. Welsh,^b R. J. Whyley,^{b,‡‡} and R. G. Winter^b

^aRutherford-Appleton Laboratory, Chilton, Didcot OX11 0QX, United Kingdom

^bCollege of William and Mary, Williamsburg, Virginia 23185

^cBoston University, Boston, Massachusetts 02215

^dUniversity of Wyoming, Laramie, Wyoming 82071

^eCalifornia Institute of Technology, Pasadena, California 91125

^fCarnegie-Mellon University, Pittsburgh, Pennsylvania 15213

(Received 26 June 1989)

A systematic experimental study of strong interaction shifts, widths, and yields from high- Z kaonic atoms is reported. Strong interaction effects for the $K^-(8 \rightarrow 7)$ transition were measured in U, Pb, and W, and the $K^-(7 \rightarrow 6)$ transition in W was also observed. This is the first observation of two measurably broadened and shifted kaonic transitions in a single target and thus permitted the width of the upper state to be determined directly, rather than being inferred from yield data. The results are compared with optical-model calculations.

The strong interaction plays an important role in hadronic atoms. Unlike muonic atoms, where the absorption on a nucleon takes place through the weak interaction, the atomic cascade of negatively charged hadrons is observed to terminate at a principal quantum number greater than 1 for all nuclei except $Z=1$. This is especially striking in heavy nuclei where a K^- meson is absorbed before reaching the $n=5$ state. The strong interaction manifests itself in three ways: The lowest observed state is both shifted and broadened, and nuclear absorption from the next higher level decreases the yield of the last observed transition.

Nuclear absorption is governed by the strength of the interaction and the overlap of the hadronic atomic wave function with the nucleus. The strong interaction between the nucleus and the orbiting kaon has been treated using a phenomenological optical potential of the form¹

$$V = -\frac{2\pi}{\mu} \left[1 + \frac{M_K}{M_N} \right] [A_{Kp}\rho_p(r) + A_{Kn}\rho_n(r)],$$

where μ is the kaon-nucleus reduced mass, M_K and M_N are the kaon and nucleon masses, ρ_p and ρ_n are the proton and neutron densities in the nucleus, and A_{Kp} and A_{Kn} are (complex) effective Kp and Kn scattering lengths. The simplifying assumptions $A_{Kp} = A_{Kn}$ and $\rho_p = \rho_n$ are often made, and the optical potential reduces to

$$V = -\frac{2\pi}{\mu} \left[1 + \frac{M_K}{M_N} \right] [\bar{a}\rho(r)].$$

The complex number \bar{a} is sometimes referred to as an effective K -nucleon scattering length. Batty,¹ in an analysis of all previous kaonic atom data, found that the value

$$\bar{a} = [(0.34 \pm 0.03) + i(0.84 \pm 0.03)] \text{ fm}$$

adequately described all shift and width measurements. These data were primarily from low and medium Z nuclei.

Kaonic and Σ -hyperonic exotic atoms in lead, tungsten, and uranium have been studied at the Brookhaven Alternating Gradient Synchrotron (AGS). The magnetic moment of the Σ^- and the masses of the K^- and Σ^- obtained from these data have been published.^{2,3} In this paper we report the results of our analysis for strong interaction effects in the kaonic atom transitions.

Kaons of momentum 680 MeV/c from the separated C4 beam ($\pi^-:K^-=9:1$) were slowed down in a Cu degrader and brought to rest in a laminar target made of sheets of natural W, Pb, or depleted U immersed in liquid hydrogen. The experiment was primarily designed to study Σ^- x rays using the stopped kaon reaction

$$K^- + p \rightarrow \Sigma^- + \pi^+ \quad (46\% \text{ B.R.})$$

to produce Σ^- . The resulting monoenergetic π^+ served as a tag for Σ^- production.² Kaonic atoms were formed by beam K^- which stopped in the target sheets. X rays from the hadronic atoms were detected by three Ge detectors,^{2,3} and were sorted into tagged or untagged histograms depending on whether or not the event was in coincidence with a π^+ . The tagged spectra primarily contained Σ^- atomic x rays, while K^- x rays dominated the untagged spectra. The Ge detector resolution, line shape, and absolute energy calibration were monitored continuously during the AGS beam spill. Accidental coincidences between beam π^- and radioactive sources were accumulated along with the data spectra. The calibration sources⁴ used were ⁵⁷Co, ¹³³Ba, ¹⁹²Ir, and ¹³⁷Cs. For the U target, additional calibration sources of ¹⁹⁸Au and ⁵¹Cr were present. During the beam-off portion of the AGS beam spill, histograms from the 122.061- and

661.660-keV lines from ^{57}Co and ^{137}Cs were accumulated. Every ten minutes these histograms were fitted on-line to provide a check on the gain stability of the system and the results were written to tape for use in the off-line analysis as a two-point stabilization correction.

Two approaches were used to study γ rays which might fall in the region of the kaonic x rays. The γ rays which were excited by beam π^- appeared in the beam-on calibration spectra along with the calibration lines. In addition, a separate study was made of γ rays produced by π^- stopping in each target. The Pb and U $K^-(8 \rightarrow 7)$ transitions were found to be free from contaminant γ lines, but there were contaminant lines present under both the $K^-(8 \rightarrow 7)$ and $K^-(7 \rightarrow 6)$ transitions in W.

The kaonic x-ray lines previously listed were fitted with the convolution of a Lorentzian and a Gaussian function, viz., a Voigt profile or Voigtian.⁵ The centroid, the natural linewidth, and the area of the Voigtian were determined by a least-squares fit to the data. In Fig. 1 the data from one detector for the W $K^-(8 \rightarrow 7)$ transition are shown along with the best fit to a Voigtian.

Once the channel number for the centroid of a Voigtian was obtained, it was necessary to convert this channel number to energy. Detailed studies of the integral nonlinearities in the detector-amplifier-analog-to-digital converter (ADC) systems revealed that nonlinearities as large as 2 parts in 10^4 were present in some energy regions. The deviation of the gain from a linear function was parametrized by up to a sixth-order Legendre polynomial for each of the three detectors.

Two different procedures to determine the energy which corresponded to a given channel number were employed. If an x-ray transition fell in a region where the residuals from a linear fit varied linearly, and calibration lines existed with energies that bracketed the line of interest, a linear interpolation was used to determine the energy of the transition. The statistical error on the transition energy from the centroid uncertainties was calculated. The weighted average of the transition energy was

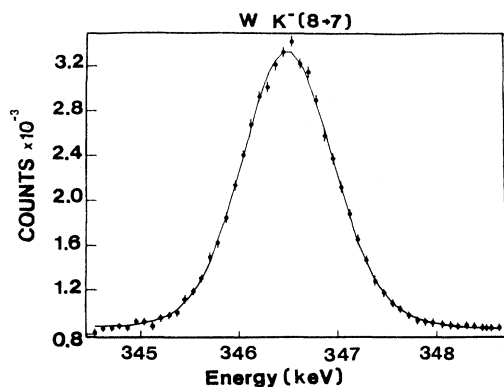


FIG. 1. The W $K^-(8 \rightarrow 7)$ transition. This spectrum comes from one detector and represents approximately 20% of the data on this transition. The smooth curve is the best fit to the data. The normalized χ^2 for the fit was 1.0.

calculated, as well as the statistical error. If the χ^2 per degree of freedom for this set was greater than 1.0, the statistical error on the average was increased³ by the factor $(\chi^2/\nu)^{1/2}$, where ν is the number of degrees of freedom. The uncertainty on the transition energy from the energy uncertainties on the calibration lines⁴ was then added in quadrature to the statistical error on the centroid. This was taken to be the total error on the transition energy. For transitions not satisfying the foregoing criteria, it was necessary to use the Legendre polynomial fit to the nonlinearities to determine the energy. Since the intensity and number of calibration lines were limited, this procedure resulted in larger uncertainties on the transition energies than were obtained from those for which the linear interpolation was appropriate.

In the spectrum obtained from stopping π^- in W, a nuclear γ ray appeared at an energy of 346.729 ± 0.030 keV. It was presumed that this same line was also present in the untagged spectrum, and therefore was present under the $K^-(8 \rightarrow 7)$ x ray. In the analysis of this x-ray transition, a contaminant γ ray was included at that energy. Its functional form was assumed to be Gaussian and the width was held fixed to the instrumental resolution. As a starting point, it was assumed that the yield of this γ ray was approximately the same per stopping K^- as it was per stopping π^- in the background run. This implied an intensity equal to 15% of the area of the $K^-(8 \rightarrow 7)$ transition. A fit to the W $K^-(8 \rightarrow 7)$ x-ray line with this contaminant intensity had a χ^2 substantially larger than fits in which the contaminant intensity was assumed to be lower. A series of fits determined that below a critical intensity (5%) for the contaminant, the χ^2 as a function of contaminant amplitude was flat. Above that amplitude it increased rapidly. In the subsequent analysis for the strong interaction width and shift, the yield of this contaminant was fixed at 5% of the $K^-(8 \rightarrow 7)$ intensity. The amplitude of the contaminant was then varied by a factor of 2 in both directions, and the change in centroid of the kaonic x ray was determined. The errors in the centroid and width of the Voigtian were then increased to include this uncertainty.

Examination of the region of the spectrum of the $K^-(7 \rightarrow 6)$ transition in W showed the presence of two nuclear γ rays (see Fig. 2). A line at 538 keV was excited by in-flight π^- and appeared in the beam-on calibration spectrum. The centroid and width of this contaminant were determined from a fit, and were held fixed in the subsequent analysis. The second contaminant γ ray did not appear in either the calibration or the stopped π^- data, although it is clearly visible in the untagged spectrum. In the analysis, it was represented by a Gaussian, and its width was held fixed to the detector resolution. Also lying under the $K^-(7 \rightarrow 6)$ transition was the $\Sigma^-(12 \rightarrow 10)$ transition. Its intensity relative to the $\Sigma^-(11 \rightarrow 10)$ transition was determined from the tagged spectrum. Its amplitude under the $K^-(7 \rightarrow 6)$ transition was then determined from this ratio and the $\Sigma^-(11 \rightarrow 10)$ intensity in the untagged spectrum. The amplitude of this Σ^- x ray was held fixed in the least-squares fit. For each of these contaminants, the yield was less than

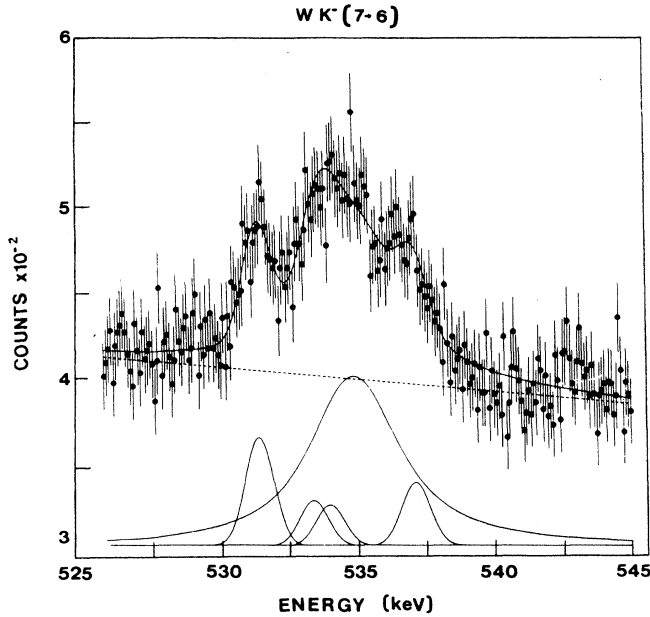


FIG. 2. The $W K^-(7 \rightarrow 6)$ transition from the same data sample as Fig. 1. In addition to this transition, two nuclear γ rays and the $\Sigma^-(12 \rightarrow 10)$ (fine-structure split) transitions are in this region. These lines were included in the fit as described in the text.

$\sim 10\%$ of the $K^-(7 \rightarrow 6)$ transition.

The relative efficiencies of the x-ray detectors and the x-ray absorption in the target were determined as a function of energy as described in Refs. 2 and 5. The area corresponding to each x-ray transition was corrected for detector efficiency and absorption in the target sheets.

A cascade calculation⁶ was used to determine the intensities of the unresolved parallel radiative transitions, e.g., the $(n=9, l=7) \rightarrow (n=8, l=6)$ transition is not resolved in energy from the $(n=9, l=8) \rightarrow (n=8, l=7)$ transition. The cascade calculation included both Auger and radiative transitions along with strong absorption, which was included using the value of \bar{a} given before. The populations of the $(n=8, l=7)$ state for W, Pb, and U, and the $(n=7, l=6)$ state for W were determined

from the measured intensities corrected by the cascade calculation. The yield was taken to be the measured radiative intensity out of the upper state divided by the total intensity into the state, which had been corrected for the ($\sim 1\%$) effective increase of the upper-state population by Auger transitions.

The calculated electromagnetic (EM) transition energies and the measured energies are given in Table I. The measured and calculated energy shifts, Lorentzian linewidths, and yields are given in Table II. The calculations are discussed in the following. The shift ΔE is defined as $E_{\text{Measured}} - E_{\text{EM}}$. The measured yield of the $W K^-(7 \rightarrow 6)$ transition implies a strong interaction width of 109 ± 27 eV for the $W K^-(n=7, l=6)$ level compared with the value of 70 ± 15 eV measured directly from the $W K^-(8 \rightarrow 7)$ transition. These data represent the first instance in which the strong interaction widths and shifts of two transitions in the same Z kaonic atom have been measured directly.

The electromagnetic kaonic transition energies in W and Pb were calculated following the method of Borie⁷ as improved by Phillips.⁸ We used the kaon mass of 493.636 MeV which was reported in Ref. 3, since the same program was used there as in this work to calculate transition energies. Because ^{238}U is a deformed rotational nucleus, there is substantial dynamic $E2$ mixing.⁹ The electromagnetic transition energy was calculated and the $E2$ correction of Chen *et al.*⁹ was added to it.

The asymmetric error on the measured Pb $K^-(8 \rightarrow 7)$ transition energy reflects uncertainties in the absolute energy calibration. These uncertainties resulted in part because the e^+e^- 511 keV annihilation line does not provide a reliable energy calibration. The energy may be shifted by an amount which depends on the specific material in which the positron annihilates.¹⁰ Different energies were obtained from the Pb $K^-(8 \rightarrow 7)$ transition depending on whether the 511 keV line was used as a calibration. The energy of this transition was determined five different ways, two of which involved using the 511 keV line. Since there was no reason to favor one method over the other, the (unweighted) mean value of the transition energies obtained from each of the five methods was used to determine the measured energy. The $\pm 1\sigma$ region was assumed to encompass the entire region covered by the individual σ 's obtained from the separate methods.

TABLE I. Measured and calculated electromagnetic K^- transition energies. In the calculation of the electromagnetic transition energies, the kaon mass was assumed to be 493.6364 MeV. This value was used since the transition energies listed below were determined from the same data as our recent measurement of the K^- mass.³ The uncertainties in the calculated electromagnetic energies are less than ± 1 eV.^{3,5} The dynamic $E2$ correction and the theoretical uncertainty on this correction were taken from Ref. 8.

Nucleus	Transition	Measured Energy (keV)	Calculated Energy (keV)
W	$8 \rightarrow 7$	346.624 ± 0.025	346.545
W	$7 \rightarrow 6$	534.886 ± 0.092	535.239
Pb	$8 \rightarrow 7$	$426.221^{+0.027}_{-0.057}$	426.149
U	$8 \rightarrow 7$	538.315 ± 0.100	538.719 ± 0.133

TABLE II. The measured and calculated strong interaction widths Γ , shifts ΔE , and yields Y for the K^- x-ray transitions. Also presented are unpublished results from Miller¹³ and a Pb $K^-(8 \rightarrow 7)$ shift derived from the data of Cheng *et al.*¹¹ The subscripts C and M stand for calculated and measured, respectively. The width Γ_M is the strong width of the lower level which was obtained by subtracting the electromagnetic widths of the upper and lower levels as well as the strong width of the upper level from the Lorentzian width obtained in the fit to a Voigtian. The parameter δ is the difference in diffusivity between the proton and neutron distributions (see text). The calculated values were obtained using the scattering length obtained in Ref. 1, $\bar{a} = [(0.34 \pm 0.03) + i(0.84 \pm 0.03)]$ fm.

Transition	ΔE_M (keV)	Γ_M (keV)	Y_M %	δ (fm)	ΔE_C (keV)	Γ_C (keV)	Y_C %
W $K^-(8 \rightarrow 7)$	$+0.079 \pm 0.025$	0.070 ± 0.015	100 ± 4	0.05	-0.003	0.065	96
W $K^-(7 \rightarrow 6)$	-0.353 ± 0.092	3.72 ± 0.35	16 ± 4	0.05	-0.967	4.187	24
Pb $K^-(8 \rightarrow 7)$	$+0.072^{+0.027}_{-0.057}$	0.284 ± 0.014	82 ± 4	0.05	-0.023	0.271	85
	$+0.032 \pm 0.012^b$	0.37 ± 0.15^a	79 ± 8^a				
U $K^-(8 \rightarrow 7)$	-0.40 ± 0.17	2.67 ± 0.10	58 ± 5	0.22	-0.189	2.531	34
	0.12 ± 0.42^a	1.50 ± 0.75^a	35 ± 12^a				

^aJ. P. Miller¹³ The shift for U was calculated with Miller's measured energy and the calculated energy in Table I.

^bCalculated with the measured energy of S. C. Cheng *et al.*¹¹ and the calculated energy in Table I.

Our measured transition energy agrees with that reported by Cheng *et al.*¹¹ as does our measurement of the Pb $K^-(9 \rightarrow 8)$ transition energy.³

The measured energy of the U $K^-(8 \rightarrow 7)$ transition does not agree with that reported in Ref. 9. However, Chen *et al.*⁹ point out that they did not have any energy calibration above the 511 keV e^+ annihilation line and thus this difference should not be considered serious.

The results from this experiment are listed along with other existing data in Table II. These results are compared to optical-model predictions with $\bar{a} = [0.34 + i0.84]$ fm as found from a fit¹ to shifts and widths in low and medium Z nuclei. Separate two-parameter Fermi distributions

$$\rho_{n,p}(r) = \frac{1}{1 + \exp \left[\frac{r - R_{n,p}}{b_{n,p}} \right]}$$

were used for the neutron and proton densities. Values for the proton distribution radius and diffusivity, R_p and b_p , were taken from de Jager *et al.*¹² Initial calculations with the same parameters for the proton and neutron density distributions generally gave results for the strong interaction width which were too small. Since kaon absorption is sensitive to the nuclear periphery, the effect of changing the parameters for the neutron distribution was investigated. Increasing R_n to fit the data gave unphysically large values, so R_n was assumed to be equal to R_p . Considerable sensitivity to the diffusivity parameter was found. With the assumption that $R_n = R_p$, the quantity $\delta = b_n - b_p$ was varied to get a good fit to the shift and width values (from this experiment) for each nucleus. These best-fit values and the corresponding δ are also given in Table II together with the calculated yields. The uncertainty in δ is typically ± 0.01 fm.

The measured strong interaction parameters are reasonably well reproduced by the present calculations

with the exception of the two shift values for W and the relative yield value for the U $K^-(8 \rightarrow 7)$ transition. If these three latter values are omitted then the value of χ^2/point for the nine remaining shift, width, and relative yield values is 1.61, which should be compared with 1.34 obtained previously¹ in the fit to low and medium Z nuclei.

A feature of the present analysis is the need to include nonzero values for δ , corresponding to an increased diffusivity b_n for the neutron densities, if a best fit is to be obtained with the value of \bar{a} which fits the low and medium Z nuclei. The values of δ , in the range 0.05–0.1 fm, correspond to differences in the rms radii of the neutron and proton distribution of 0.07–0.16 fm which seem to be physically very reasonable. This suggests that a single value for \bar{a} can be used throughout the periodic table, providing the difference in neutron and proton distributions is taken into account by increasing the value of the neutron diffusivity.

Finally we should comment on the positive shift values measured for the W $K^-(8 \rightarrow 7)$ and Pb $K^-(8 \rightarrow 7)$ transitions. These values cannot be reproduced with the present form of the optical potential when it is required to fit data for lighter nuclei. A similar effect has also been seen in antiprotonic atoms where a positive shift value for antiprotonic ^{174}Yb has been measured in two separate experiments.^{14,15}

ACKNOWLEDGMENTS

We gratefully acknowledge the efforts of R. Pehl, F. Goulding, D. Landis, N. Madden, and R. Trammell in developing the Ge detector system. We thank D. Lazarus, D. Lowenstein, and the AGS staffs for their support. We thank R. Meier and the hydrogen target group for the construction of the laminar target, and E. J. Austin, G. W. Dodson, J. Ginkel, D. Joyce, C. Kenney, J.

Kraiman, and D. R. Tieger for their participation in portions of the experiment. We thank J. Reidy and R. Helmer for helpful discussions on absolute energy calibration and E. Borie, M. Leon, and R. Seki for the use of their

computer codes. This work was supported in part by the U.S. National Science Foundation, the U.S. Department of Energy, and the United Kingdom Science and Engineering Research Council.

*Present address: Department of Radiation Medicine, Massachusetts General Hospital, Boston, MA 02114.

†Present address: EG&G, Energy Measurements, Box 380, Suitland, MD 20746.

‡Present address: Department of Physics, University of Illinois, Urbana, IL 61801.

§Present address: AT&T Bell Laboratories, Whippany, NJ 07981.

**Present address: Bell Communications Research, Red Bank, NJ 07981.

††Present address: Institut für Physik der Universität Basel, CH-Basel 4056, Switzerland.

‡‡Present address: MCI Telecommunications Corp., McLean, VA 22102.

¹C. J. Batty, Nucl. Phys. A **372**, 418 (1981).

²D. W. Hertzog, M. Eckhause, P. P. Guss, D. Joyce, J. R. Kane, W. C. Phillips, W. F. Vulcan, R. E. Welsh, R. J. Whyley, R. G. Winter, E. Austin, J. P. Miller, F. O'Brien, B. L. Roberts, G. W. Dodson, R. J. Powers, R. B. Sutton, and A. R. Kunselman, Phys. Rev. D **37**, 1142 (1988).

³K. P. Gall, E. Austin, J. P. Miller, F. O'Brien, B. L. Roberts, D. R. Tieger, G. W. Dodson, M. Eckhause, J. Ginkel, P. P. Guss, D. W. Hertzog, D. Joyce, J. R. Kane, C. Kenney, J. Kraiman, W. C. Phillips, W. F. Vulcan, R. E. Welsh, R. J. Whyley, R. G. Winter, R. J. Powers, R. B. Sutton, and A. R. Kunselman, Phys. Rev. Lett. **60**, 186 (1988).

⁴A. Lorentz, *Nuclear Decay Data for Radionuclides used as Calibration Standards*, IAEA Nuclear Data Section, Report No. INDC(NDS)-145/GEI, 1983.

⁵B. L. Roberts, R. A. J. Riddle, and G. T. A. Squier, Nucl. Instrum. Methods **130**, 559 (1975); **144**, 369 (1977); C. J. Batty, S. D. Hoath, and B. L. Roberts, *ibid.* **137**, 179 (1976).

⁶The code used was written by Leon and Seki and is described in M. Leon and R. Seki, Phys. Rev. Lett. **32**, 132 (1974).

⁷E. Borie, Phys. Rev. A **28**, 555 (1983).

⁸W. C. Phillips, Ph.D. thesis, College of William and Mary, 1988 (unpublished).

⁹M. Y. Chen, Y. Asano, S. C. Cheng, G. Dugan, E. Hu, L. Lidofsky, W. Patton, C. S. Wu, V. Hughes, and D. Lu, Nucl. Phys. A **254**, 413 (1975).

¹⁰J. Reidy (private communication); R. Helmer (private communication).

¹¹S. C. Cheng, Y. Asano, M. Y. Chen, G. Dugan, E. Hu, L. Lidofsky, W. Patton, C. S. Wu, V. Hughes, and D. Lu, Nucl. Phys. A **254**, 381 (1975).

¹²D. W. de Jager, H. De Vries, and C. De Vries, Atom. Nucl. Data Tables **14**, 479 (1974).

¹³J. P. Miller, Ph.D. thesis, Carnegie-Mellon University, 1974.

¹⁴P. Robertson, T. King, R. Kunselman, J. Miller, R. J. Powers, P. D. Barnes, R. A. Eisenstein, R. B. Sutton, W. C. Lam, C. R. Cox, M. Eckhause, J. R. Kane, A. M. Rushton, W. F. Vulcan, and R. E. Welsh, Phys. Rev. C **16**, 1945 (1977).

¹⁵A. Kreissl, A. D. Hancock, H. Koch, Th. Köhler, H. Poth, U. Raich, D. Rohmann, A. Wolf, L. Tauscher, A. Nilsson, M. Suffert, M. Chardalas, S. Dedoussis, H. Daniel, T. von Egidy, F. J. Hartmann, W. Kanert, H. Plendl, G. Schmidt, and J. J. Reidy, Z. Phys. A **329**, 235 (1988).